

Pile Design and Group Behaviour; A Case Study of Large Tank Foundations in Soft Soil Conditions

W.F. Van Impe^{1,2}, P.O. Van Impe¹ and A. Manzotti³

¹AGE Consultants bvba, Erpe-Mere, Belgium

²Ghent University, Ghent, Belgium

³Alice Manzotti engineering, Ghent, Belgium

E-mail: william.vanimpe@ugent.be

ABSTRACT: The paper presents the case study on the construction of three 48m diameter oil tanks in Ostend (Belgium), each founded on a group of 422 displacement cast in-situ screw piles. The three tanks are close enough to each other to induce interaction. Monitoring of the tanks' movements has been performed during the hydro-testing of the steel tanks and during the subsequent working stage of the tanks. The bearing layer of the pile group is a 5m thick stiff sand layer at a depth of about 20m, overlain by a very heterogeneous soft clayey/silty fill containing sand pockets, and underlain by a very thick slightly over-consolidated clay. Some short and long term settlement prediction of the tanks have been done, assuming soil parameters derived from the CPT data on site, and compared to the measured settlements. The initially derived soil parameters are then re-evaluated in order to predict the long term settlement for the full life span of the construction.

KEYWORDS: Pile group, Screw pile, Group effect, Load-settlement behavior, Oil tanks, Pile loading testing, Residual stress

1. INTRODUCTION

1.1 The oil tanks' foundation case study

The main geotechnical issue with the design of oil tanks is that, today, fuel tanks very often are being erected in harbour sites with poor soil conditions. In harbour area, the soil often consists of quite thick soft alluvial clayey-, silty clayey- and peaty-layers.

In order to solve the foundation problems in such soil conditions, three main solutions are possible: 1) starting from a deep foundation concept; 2) preconsolidating (improving) the soft layers with temporary overburden or with vacuum consolidation principles, combined with vertical drains to accelerate and improve the consolidation process; either 3) establishing the tank directly on a well-designed artificial embankment on the soft layers, installing hydraulic jacks to adjust continuously for the differential and absolute settlements.

The case study which will be presented here in this paper refer to three oil tanks located in Ostend (Belgium), steel structures of 48 m in diameter and 19 m height, each containing 33000 m³ and positioned in a triangular shape at a center-to-center interdistance of about 65 m (Figure 1 and Figure 2). They are founded on a 48.8m diameter, 60 cm thick reinforced slab, supported by 422 displacement screw piles.



Figure 2 Fuel tanks under construction at Ostend (Belgium) – fall of 2012.

The 460 mm diameter displacement screw piles of the Omega pile type (Figure 3) are placed at an interdistance of 2.2 m (centre-to-centre) and reach to a depth of 21.5 m. They have been designed, with a global safety of about 2, according to the Van Impe-De Beer (1986) method to each take a maximum design load of 960 kN, including some 180 kN negative skin friction load. The actual unit overburden load of a fully loaded tank with foundation slab is indeed rising up to about 220 kN/m², determining a total foundation load still to be increased by some negative skin friction loading. Such negative skin friction up to at most 17 m depth, originates from the reconsolidation of the soft layers along the pile shaft, as a result of the remolding by the pile group installation itself.

The conclusion is that the foundation design of the oil tanks can actually be considered as a foundation on a large group of about 400 end bearing displacement screw piles, cast in situ, until about 22 m of depth. The ultimate pile tip capacity (about 1750 kN), at the optimum pile tip level, can be increased with the ultimate pile shaft capacity in the about 3.5 m bearing sand layer situated above the pile tip (about 200 kN), to reach a full total ultimate pile capacity of about 1950 kN and so the allowable capacity of >960 kN.

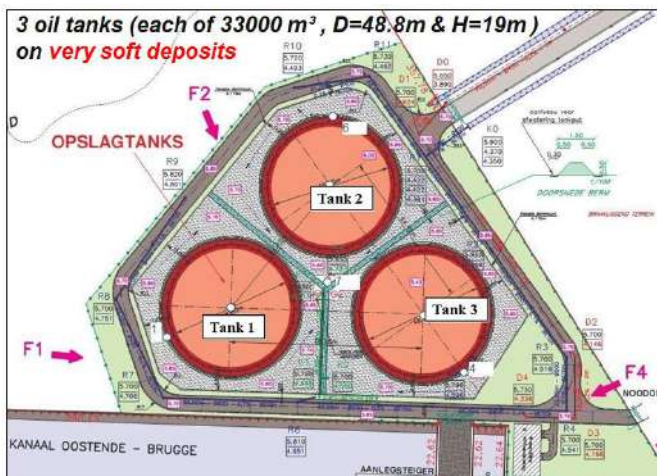


Figure 1 Overview of the site and location of the three tanks at Ostend (Belgium).

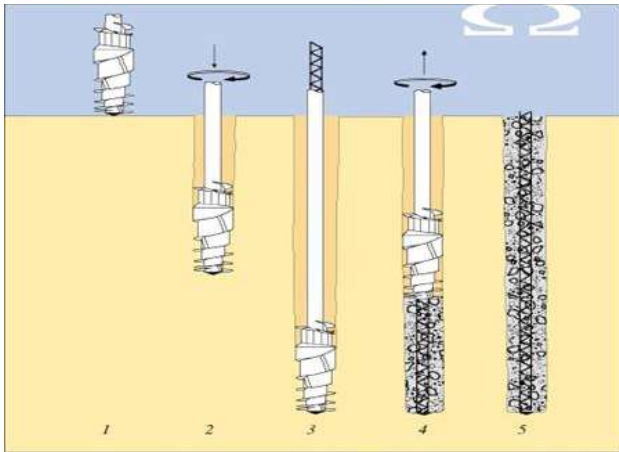


Figure 3 The Omega screw pile type in Belgium.

1.2 Soil conditions at the site

The soil conditions, up to depths of roughly 12 to 15 m can be described as very heterogeneous fill consisting of a very soft clayey/silty material containing sandy lenses (Figure 4). The location and thickness of these lenses vary considerably across the site (Figure 5 and 6).

The whole area where the tanks are located seems to be excavated and hydraulically refilled over decades, before reaching the today's new destination of the site as an oil tank plant. It means that below some thin or weaker quaternary soil lenses, from about 12–15 m up to depths of about 18-19.5 m, the first natural bearing layer would be the very dense tertiary sand with a very consistent thickness of about 4-5 m. The piles are installed to about 1.5m into the sand layer.

This foundation layer is underlain by a silty clay which reaches down to the depth of 45 m as suggested by geological data. This silty clay layer is itself underlain by a very large over-consolidated clay layer reaching depths of 170m. This clay resembles to some extent the London clay.

The large number of CPT tests which have been performed at the site confirm the heterogeneity of the fill and the quite regular location and thickness of the tertiary sand.

Unfortunately, none of these CPTs was reaching more than 10m into the silty clay layer, making impossible to define its actual thickness or to get any information on the thick O.C. clay layer of the formation below.

Figures 7, 8 and 9 represent a typical CPT on the site and the corresponding soil type classification and stiffness parameters'

estimation as by Robertson 2010 (Young's modulus E, constrained modulus M and small strain shear modulus G_0) (Table 1).

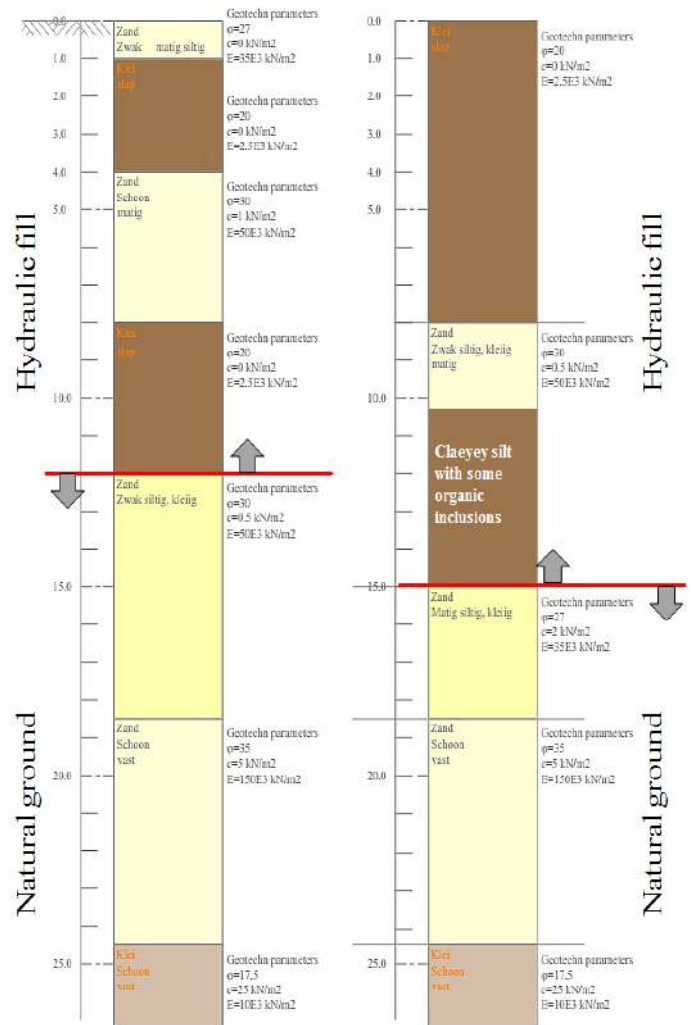


Figure 4 General overview of typical bore profiling outcome at the oil tank site.

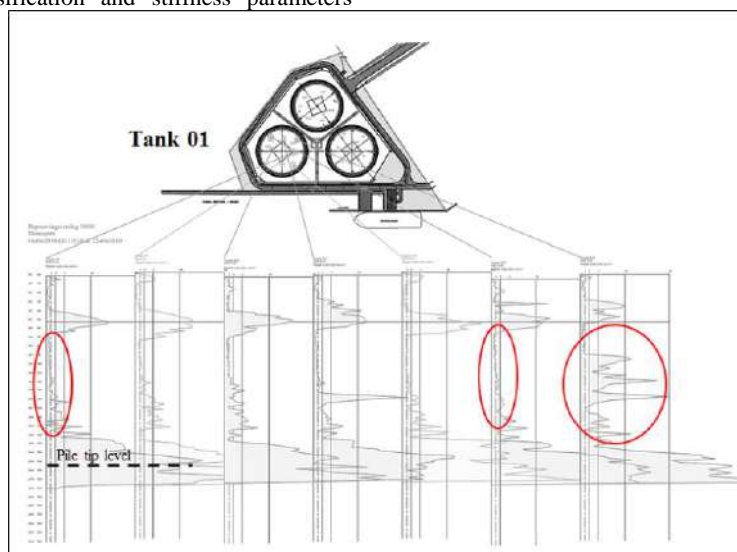


Figure 5 Pattern of soil resistance variability under Tank 1.

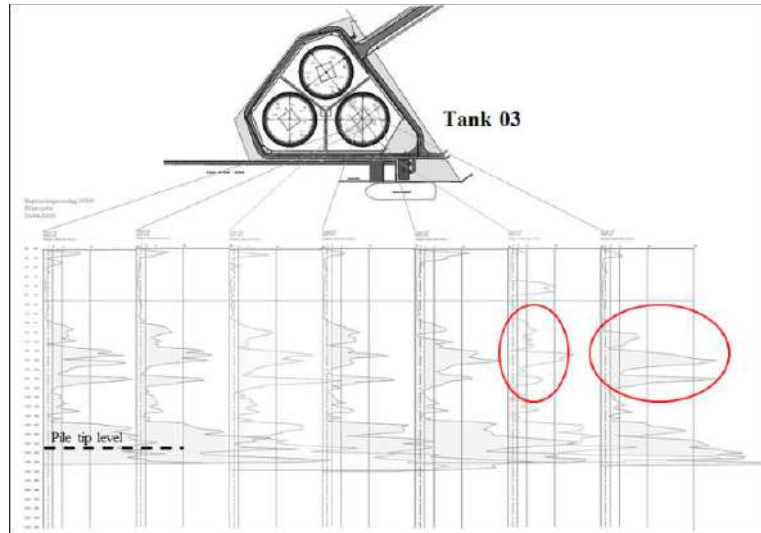


Figure 6 Pattern of soil resistance variability under Tank 3.

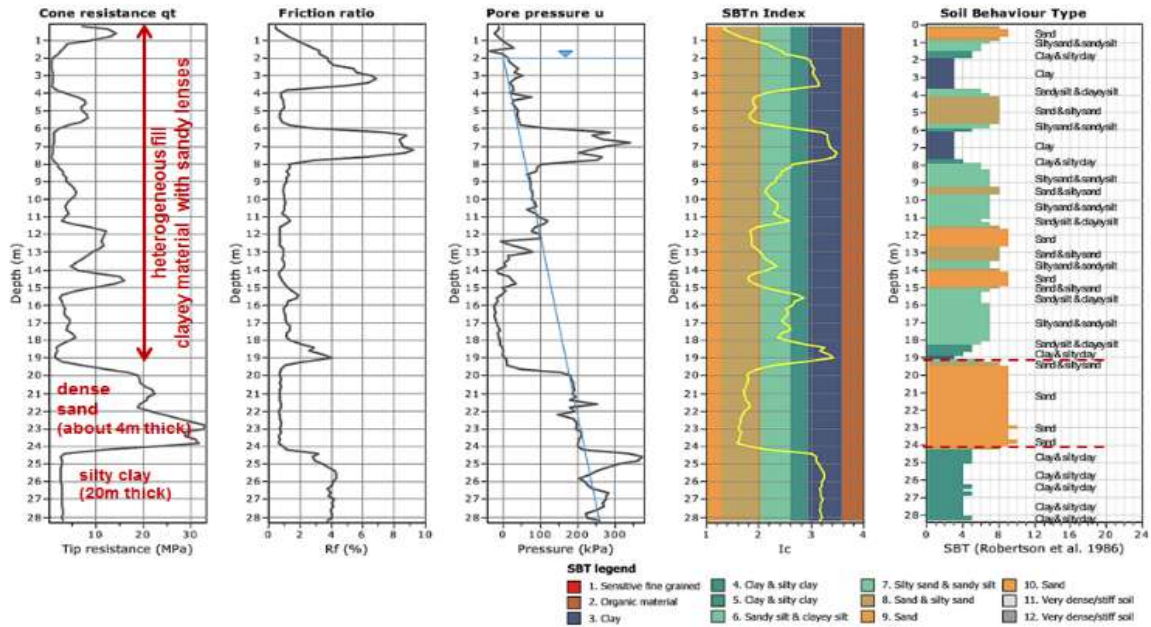


Figure 7 Typical CPTu profile in the area of the oil tanks in Ostend.

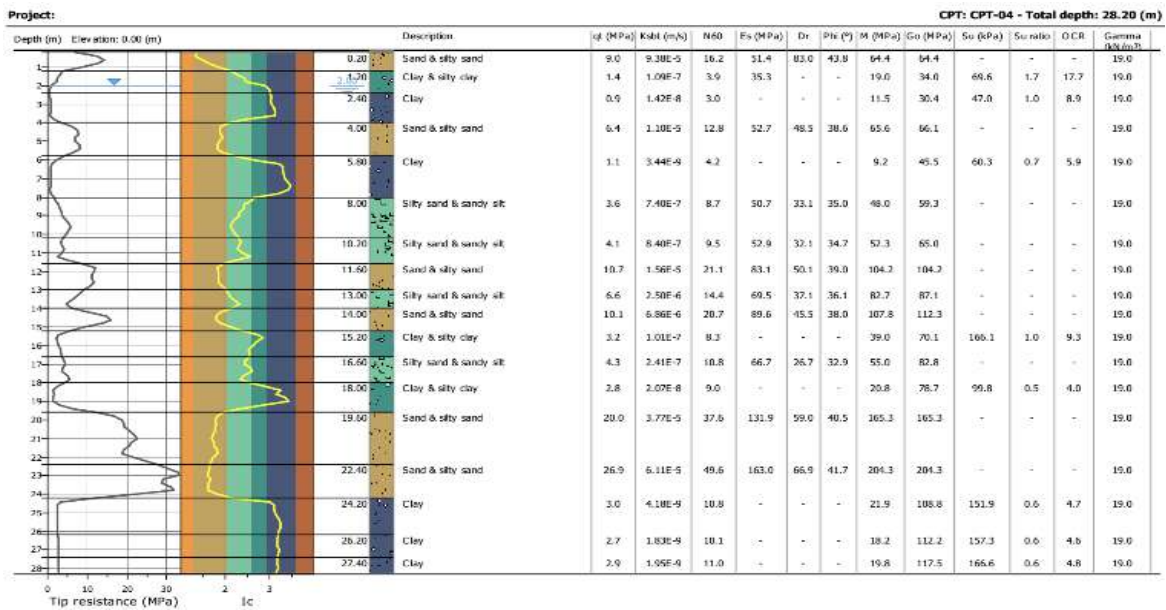


Figure 8 Example of soil data estimation from CPT interpretation (Robertson 2010).

The bearing sand layer does show CPT cone resistances of about 20 MPa, with peaking resistance over 30 MPa in some cases, while the slightly O.C. clay layer underneath, in the upper part, slowly varies its cone resistance with depth, from about 2.5 to 5 MPa (Figure 7-9 and Table 1).

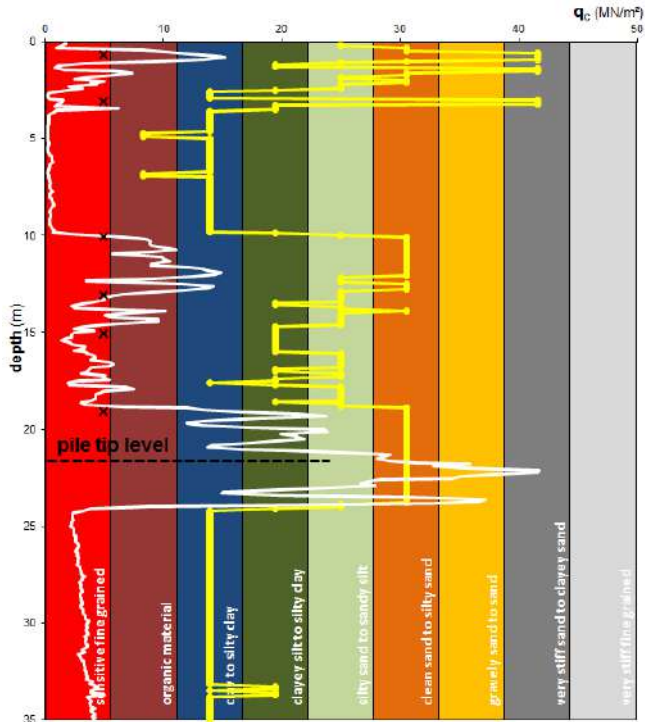


Figure 9 CPT based soil type classification (q_c profile: white line; SBTn : yellow line, Robertson 2010) at the location of the test pile axis. The black crosses represent the locations of the 6 extensometer.

Table 1 Estimated stiffness parameters from the CPT result at the test pile location (Robertson, 2010).

Depth (m)	q_c (MPa)	E (MPa)	M (MPa)	G_0 (MPa)
0.66	4.60	34	40	45
3	0.66	4	5	23
10	10.07	77	97	97
14.5	5.28	63	66	80
18	15.80	118	143	147
21.56	35.68	225	282	282
22.48	26.18	170	209	214
24	3.3	27	27	114
35	5.23	51	51	156

2. INSTRUMENTED SINGLE PILE LOAD TEST

2.1 Ground conditions at the test pile location

In order to optimize the design method, a fully (extensometer) instrumented test pile was installed (Figure 10 to 12) to be test loaded up to a pile base settlement of 10% of the pile base diameter; which in accordance to the Belgian practice is corresponding to the required deformation at “failure load” of a soil displacement pile.

The ground conditions at the (21.56 m long) test pile axis location is given in Figure 9; at the site the ground water table can be assumed at about 0.5 m below natural ground level. The pile base is anchored in the tertiary dense sand layer, overlying the tertiary slightly O.C. 100 m thick clay formation, starting from about 2.5 m ($>5\phi_{pile}$) below the pile tip. The 6 extensometers are located at the depths shown in Figure 9.



Figure 10 Omega pile installation, test pile instrumented on the reinforcement cage at 6 depth locations.

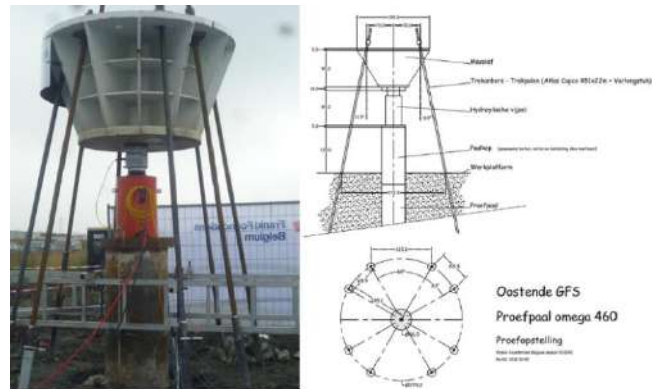


Figure 11 Test pile loading system, with 8 deep anchors inclined at 12°, each enabling a 500 kN tensile force.

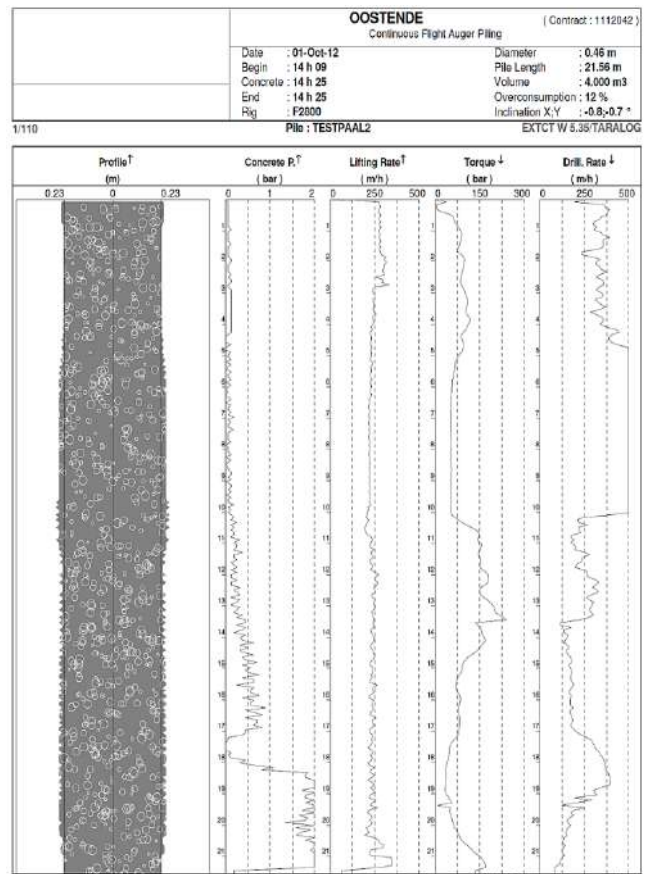


Figure 12 Test pile installation parameters of the Omega test pile.

2.2 Prediction of the pile capacity according to an adapted Belgian method

The unit ultimate pile base (460 mm diameter) capacity (method Van Impe-De Beer- 1986) times the pile base area, (cfr Figure 13-14), increased by the ultimate pile shaft capacity on the lower part of the pile shaft mainly, has been applied in order to predict the total ultimate pile capacity of the test pile. The result of this ultimate total pile capacity (Q_{ult}) prediction, linked to the CPT result at the location of the test pile is shown in Figure 15.

Ultimate base resistance

$$R_{bu} = \beta \cdot \alpha_b \cdot \varepsilon_b \cdot q_{bu}^{(m)} \cdot A_b = \beta \cdot \alpha_b \cdot \varepsilon_b \cdot Q_{bu}$$

$$\beta = 1,0$$

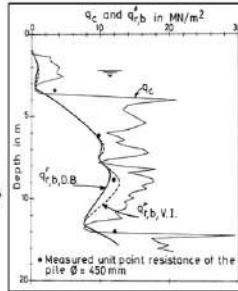
α_b = installation factor

ε_b = parameter for stiff clays

$q_{bu}^{(m)}$ or $q_{r,b}$ = ultimate unit pile base resistance

(Van Impe/ De Beer method -1986)

A_b = nominal pile base cross section area



Ultimate shaft resistance

$$R_{su} = \xi_f \cdot X_s \cdot \sum H_i \cdot q_{su,i} = \xi_f \cdot X_s \cdot \sum H_i \cdot \eta_p^* \cdot q_{c,i}$$

ξ_f = pile installation factor = 1.0

η_p^* = soil parameter, here in the tertiary dense sand: 1/150

$q_{c,i}$ = cone resistance at the considered depth i

H_i = pile shaft height corresponding to the considered layer i

X_s = pile shaft perimeter

Figure 13 The ultimate pile capacity, from CPT testing - the Belgian practice (Eurocode National application document).

At the test pile base level (21.56 m depth) such capacity prediction would consequently lead to a values of: total ultimate pile tip capacity of 2168 kN; total ultimate shaft capacity of 1943 kN. This results in a total ultimate pile capacity of $Q_{ult} \sim 4.1$ MN. The above mentioned pile shaft capacity prediction, from CPT, in this case however should be interpreted cautiously, since the pile installation itself in this type of soil heterogeneous fill material is highly sensitive to re-consolidation and so even to negative skin friction effects. It means that the upper 11 m of the shaft capacity contribution in accordance with this CPT result is highly questionable and should not be taken into account.

The only reliable positive shaft capacity contribution one can count on would be the capacity from the layer in between 11 m and 21 m depth, above the pile tip. This would in our opinion finally lead to an adapted total ultimate pile capacity Q_{ult} of 2168 kN + 1400 kN \sim 3500 kN.

2.3 Estimated stiffness moduli relevant to the pile test load

The casted concrete quality (C30/37), including the pile reinforcement cage and the extensometer cage as instrumentation of the test pile, was bringing us at an estimate of the test pile concrete stiffness of $E_c = 32000$ MPa. The test pile concrete block on top (from level -0.46 m to $+1.04$ m) would have a stiffness of 30 GPa.

The stiffness values estimated for the various soil layers identified (cfr Figure 9) along the pile shaft and underneath the pile tip at the test pile location, are summarized in Table 1.

The predicted pile load-settlement curve (Van Impe W.F. -1986, 1994), using the above mentioned stiffness estimates and the failure criterion of Q_{ult} at 10% pile tip settlement, would bring us to a value of about 3350 kN (Figure 16).

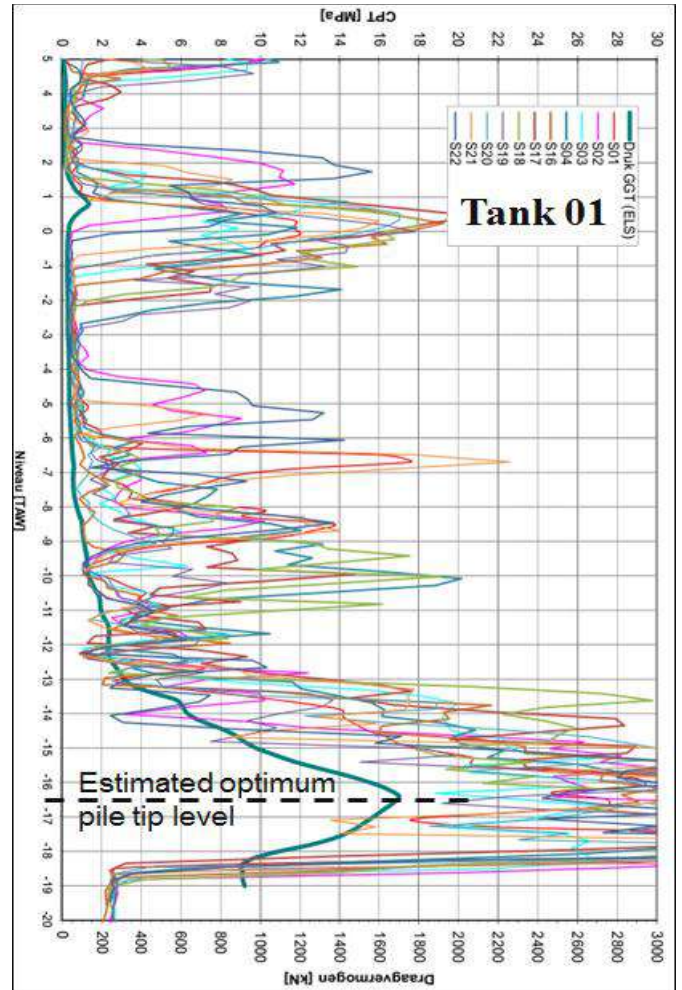


Figure 14 Examples of typical CPT-results in the area of Tank 1 and its derived total ultimate pile tip capacity at corresponding levels of possible pile tip depths (cfr Belgian practice).

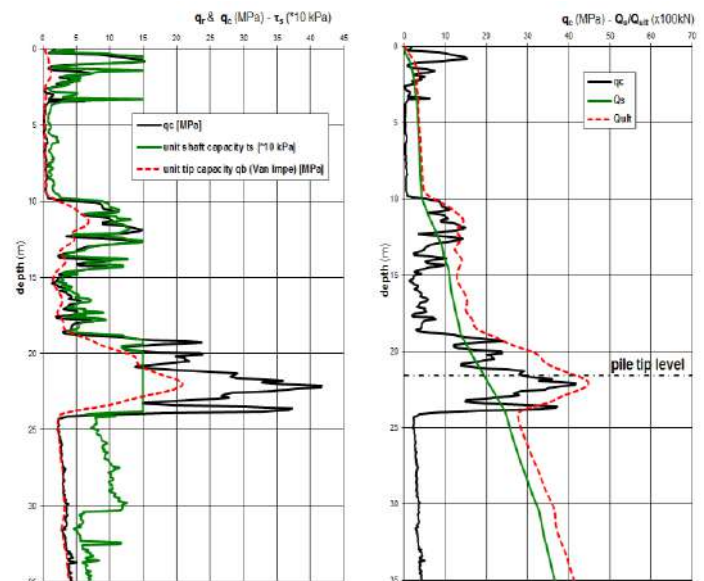


Figure 15 On the left: the unit pile tip and unit pile shaft values; on the right: the total ultimate pile capacity Q_{ult} vs depth at the location of the test pile axis.

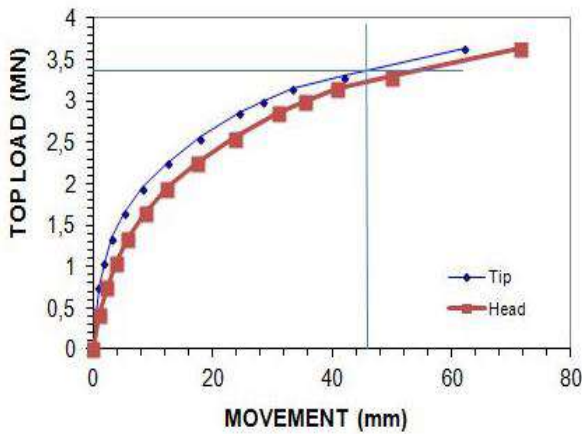


Figure 16 Estimated total ultimate pile capacity from the predicted pile load-settlement curve (Van Impe W.F. 1986–1994).

2.4 Measured load-settlement data of the test pile and corresponding capacity discussion

The actual test pile stiffness evaluation was performed on the basis of the proposal of Fellenius (2001) of plotting $\Delta\sigma/\Delta\varepsilon$ at the locations of each of the extensometers in the pile shaft, versus the local strain ε at that respective locations. Figure 17 is showing these results. All curves measured during the pile load test seem to more or less converge at values of $\Delta\sigma/\Delta\varepsilon$ of 6, corresponding to a pile stiffness of about 30 GPa; which is not so far from the first estimate we made at the start of the pile installation (32 GPa).

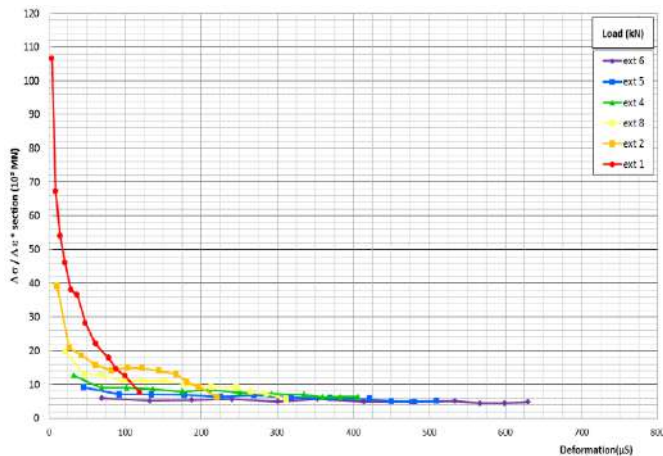


Figure 17 Stiffness evaluation of the test pile with best fit for all extensometers (adapted from Fellenius 2001 method).

Starting from the pile stiffness evaluated now from the pile test, we can draw the load distribution in the pile at the extensometer locations for the increasing pile head load levels during the load testing of the pile. Figure 18 and 19 are showing the measured data interpreted in this way. From the measured data one could read that the large deformations (>46 mm = 10% of the pile tip diameter) of the pile tip, with subsequent ongoing pile tip displacements do appear at pile head load levels in between 3300 kN and 3600 kN. This is fairly well corresponding to the CPT- predicted “failure” load of about 3.5 MN, and to the from predicted load-settlement curve ultimate load of 3.35 MN, all mentioned above.

One has to remind that all of such predictions do start from the assumption of a perfect pile soil interaction corresponding to the assumed installation factors implemented in the design method (cf Figure 13).

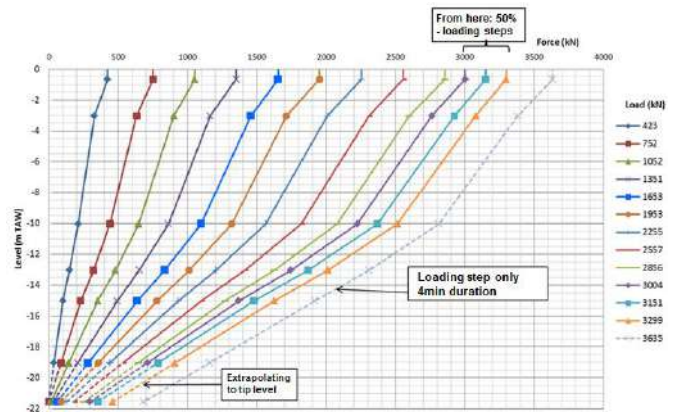


Figure 18 Axial load distribution in the test pile at the extensometer levels, and extrapolated to the pile base level.

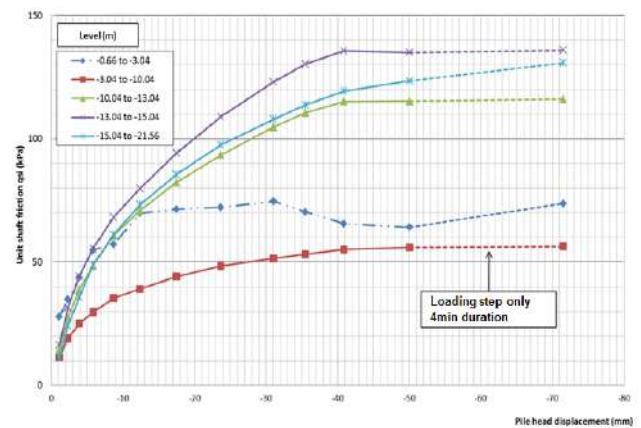


Figure 19 Mobilizing the pile shaft capacity at increasing pile deformations, in the sections in between the extensometer levels.

Even with the ultimate test pile load corresponding quite well to the predicted values, the distribution of the ultimate pile tip load versus the ultimate pile shaft load as measured appears to be quite different from the predicted distribution, discussed above under 2.2. The expected shaft capacity to be developed starting from the CPT results at the test pile location, as compared to the measured values during the test loading of the pile is indicated in Figure 20.

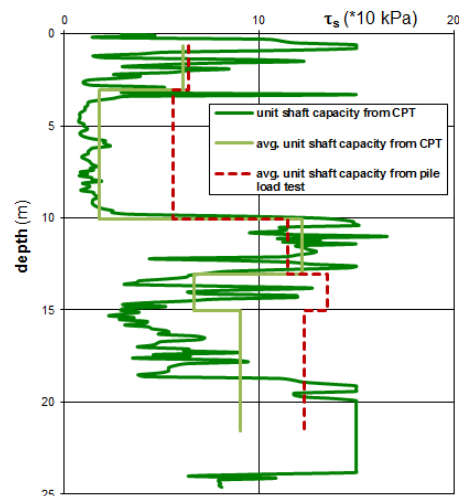


Figure 20 Comparison of the mobilized unit shaft friction along the test pile shaft; CPT based predicted mobilized friction versus the measured values during the load test.

The rather low tip bearing capacity mobilized during the pile test load can be partly explained by the indeed too weak soil- pile tip interaction at the base, caused by the long reinforcement cage with inner extensometer cage, both fitting only narrowly inside the rather small diameter opening left open by the re-screwed auger head during the casting of the concrete. The concrete flow in such case is not satisfying the requirements for a good soil-pile tip interaction. In the standard screw pile execution of this type of pile, the reinforcement cage is never reaching the pile tip level, and obviously there is no supplementary cage for the instrumentation.

The typical S-shaped load-distribution curve, and so the connected over-estimation of the unit pile shaft friction in the upper layers, is a result of induced residual strains (and stresses) in the pile due to installation procedures in the specific soil conditions (Fellenius 2002). The zero readings of the instrumentation in the pile, after the residual strains were developed, do obviously influence the interpretation of the load-settlement curves of a pile assumed to start from zero initial stress levels at zero pile head loading. The residual loads indeed quite present here, could be linked to the reconsolidation, due to pile installation effects, of the softer layers (from 4 m till 10 m depth, and from 14.7 m till 17 m depth) and consequently resulting from the negative skin friction mobilized in the entire soil layer in between 1 m and 17 m depth.

The Figure. 21 indicates with the full blue line, the test pile load distribution during the test loading at a level of 3005kN pile head load (of the assumed not pre-stressed pile). The violet dashed line indicates the negative skin friction developed along the pile shaft due to reconsolidation of the soil layer in between 1 m and 17 m depth

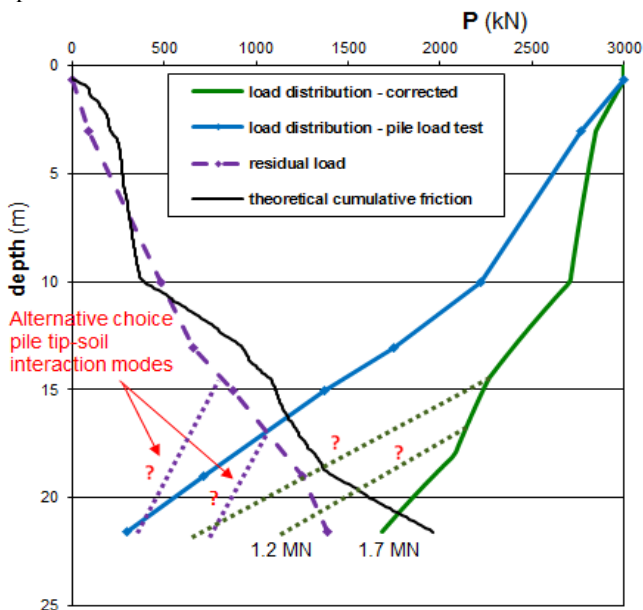


Figure 21 Corrected test pile load distribution implementing the residual stress induced loading

This is, consequently, the new zero-reference line for the extensometer readings. The actual, corrected pile load distribution curve therefore would be the full green line in Figure 21, reflecting indeed the much higher pile tip load contribution and the expected ratio pile shaft to pile tip load as one would derive from the CPT-based or the rational load-settlement curve based predictions, and leading to a pile base load of about 1.7 MN at a pile head load of 3 MN (so with a shaft load contribution of 1.3 MN).

The dashed violet line is calculated starting from the assumption of a perfect soil-pile tip interaction, which is not necessarily the case for this instrumented test pile, as argued before. So, the dotted lines in Figure 21 do suggest other possible shape developments of the dashed violet curve, including some influence of a less perfect soil-

pile tip interaction. The most reliable correction of this type in our opinion is the correction shown by the dotted line from level -17 m on. This would lead to a tip load of about 1.2 MN at a pile head load of 3 MN; so with a shaft load contribution of 1.8 MN.

Only the from lab testing derived stiffness of the soil underneath the already installed pile tip, would lead to more reliable outcome of the pile tip interaction stiffness required to optimize the interpretation of the load-distribution curve measured during the pile load test. Without this our theoretical modelling cannot be calibrated to the pile load test outcome as such, because the unknown parameters, already mentioned, in the equation still prohibit a unique solution of the in-verse problem to solve.

But, the outcome of this pile load test is anyhow showing clearly that the total ultimate pile load is – even with safety factors over $F > 3$ – satisfying largely the design load and also confirms that the expected load settlement stiffness at design load satisfies the criterion of pile tip deformations of about 3 mm at 1.5 times the design load. The ratio of the pile shaft to pile tip mobilization at ultimate capacity loading level seems to be about 0.65 to 0.7, from the corrected test results, corresponding quite well with all CPT based predictions.

2.5 Load-settlement data of the test pile and corresponding pile group deformation discussion

A very simple approach of evaluation safely the expected pile group settlements from the unique pile load-settlement behavior and with the stiffness parameters safely evaluated from the CPT test results, as for example done for the test pile in Table 1, would be to go out from an “equivalent raft” principle.

The pile group should be replaced by an equivalent raft located at a depth which depends on the nature of the soil profile and ranges from $2/3L$ for friction pile groups to L for groups of firmly end bearing piles, where L is the pile length. The load is spread at an angle which varies from 1 in 4 for the former case, to zero for the latter case. We assumed an equivalent raft at 18.16 m depth, with an equivalent out-spread diameter of 54,29 m and under an equivalent load at that depth of about 170 kPa.

The values of the constrained modulus (M) which have been used within this analysis were obtained from the CPT results, assuming certain compressibility parameters for the layers below 35m depth for which we had no data.

This method would give us a safe estimate of an upper level of the overall elastic oil tank deformation of 27 mm, to be increased by an upper level of the soil plastic deformations of about 110 mm, due to the consolidation effects of the relevant interfering layers into the foundation engineering problem. We went out for this elastic deformation estimate of the pile group, from the stiffness interaction between pile tip and soil as we could derive from the pile test loading. It's however expected that the piles at the locations of the oil tanks – having no reinforcement cage up to the pile base nor a cage for pile instrumentation - would show a stiffer pile base-soil interaction. This would bring down the expected pile group deformations. In addition, the in reality expected elastic deformations during the very short time hydro-test (it takes at most a 4 days full load) at tank loading, in our views should be lower. All the above together, the deformations during the hydro testing therefore can be expected to become for example of the order of about 70% of the previous elastic longer term values. The mentioned lasting plastic deformations due to consolidation effects are much more difficult to judge, since we don't have enough consolidation parameter information measured in the lab of the 100 m thick tertiary clay underneath the tank foundation sand layer at the tank location.

In addition, the interaction of the 3 tanks' loading, since they are only at 65 m axis-to-axis interdistance, leads unavoidably to a settlement trough as we even during the hydro testing already could notice to some extent. Settlement monitoring of the tanks was therefore deemed to be essential.

Table 5 Measured settlement (mm) of the tanks during operation (P=141 kPa): Tank 01.

Measured point	30-01-2014	26-09-2014	28-06-2015
T101	-38,30	-46,63	-49,50
T102	-39,68	-48,75	-51,75
T103	-40,84	-50,50	-53,61
T104	-41,34	-50,36	-53,53
T105	-41,93	-49,42	-52,39
T106	-38,24	-45,40	-47,50
T107	-38,12	-44,01	-46,09
T108	-36,24	-41,26	-42,63
T109	-33,60	-38,81	-39,34
T110	-33,94	-38,26	-38,79
T111	-34,40	-38,38	-39,36
T112	-33,04	-37,21	-38,32
T113	-32,00	-37,61	-37,95
T114	-33,70	-38,57	-40,57
T115	-34,57	-41,68	-43,50
T116	-36,37	-43,80	-47,00

Table 6 Measured settlement (mm) of the tanks during operation (P=142 kPa): Tank 02.

Measured point	30-01-2014	26-09-2014	28-06-2015
T201	-31,61	-42,98	-45,37
T202	-33,15	-44,99	-47,82
T203	-34,82	-47,50	-50,53
T204	-36,03	-48,69	-52,05
T205	-37,54	-50,76	-54,55
T206	-39,56	-53,58	-56,91
T207	-40,21	-54,61	-59,13
T208	-39,52	-54,24	-58,62
T209	-38,77	-52,46	-56,55
T210	-37,58	-51,40	-55,71
T211	-35,60	-49,62	-53,36
T212	-34,37	-47,16	-50,20
T213	-32,18	-44,31	-47,37
T214	-31,38	-42,84	-45,88
T215	-31,21	-42,99	-45,39
T216	-31,13	-42,64	-45,79

Table 7 Measured settlement (mm) of the tanks during operation (P=144 kPa): Tank 03.

Measured point	30-01-2014	26-09-2014	28-06-2015
T301	-48,01	-58,74	-62,44
T302	-45,17	-56,20	-59,55
T303	-44,13	-53,65	-56,61
T304	-37,02	-47,21	-49,34
T305	-40,37	-49,26	-51,78
T306	-37,42	-45,70	-48,01
T307	-34,87	-43,09	-45,83
T308	-36,22	-44,16	-46,17
T309	-31,03	-38,08	-40,32
T310	-31,01	-39,01	-41,77
T311	-29,43	-38,14	-40,65
T312	-32,47	-41,46	-44,48
T313	-33,16	-43,43	-46,70
T314	-41,97	-53,17	-56,74
T315	-49,60	-61,46	-65,41
T316	-47,60	-59,92	-63,71

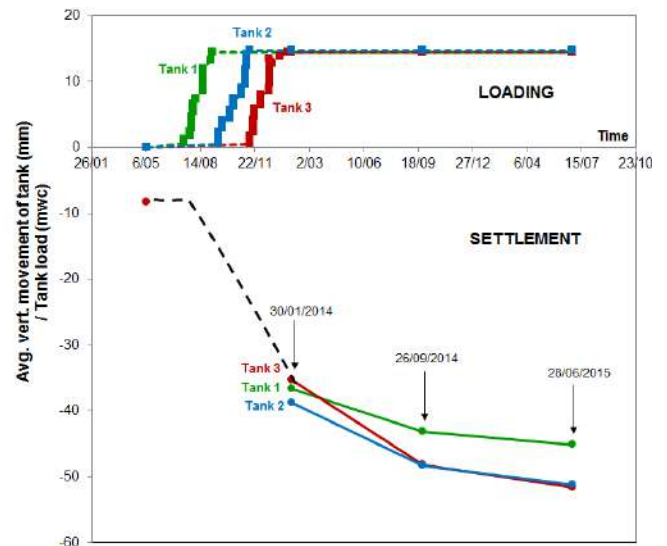


Figure 24 Average settlement (mm) of the tanks during operation.

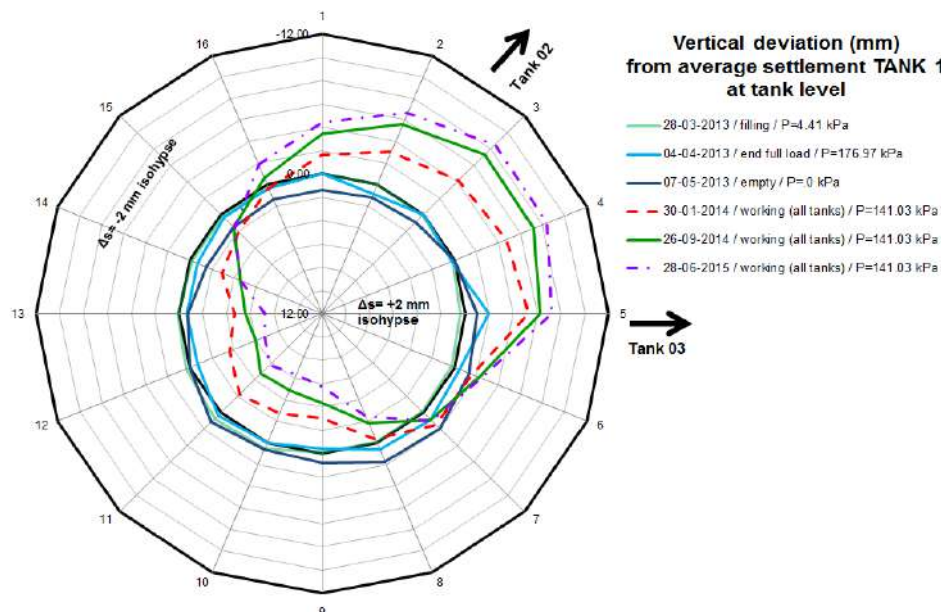


Figure 25 Vertical deviation from average settlement (mm) of Tank 1 - during hydro test and during operation, at tank level.

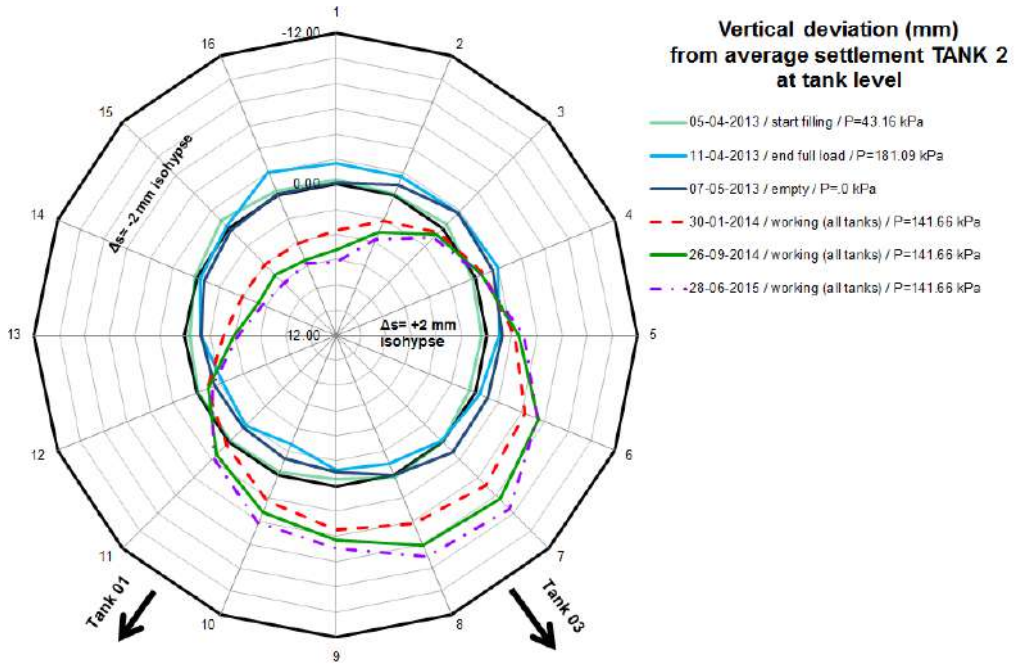


Figure 26 Vertical deviation from average settlement (mm) of Tank 2 - during hydro test and during operation, at tank level.

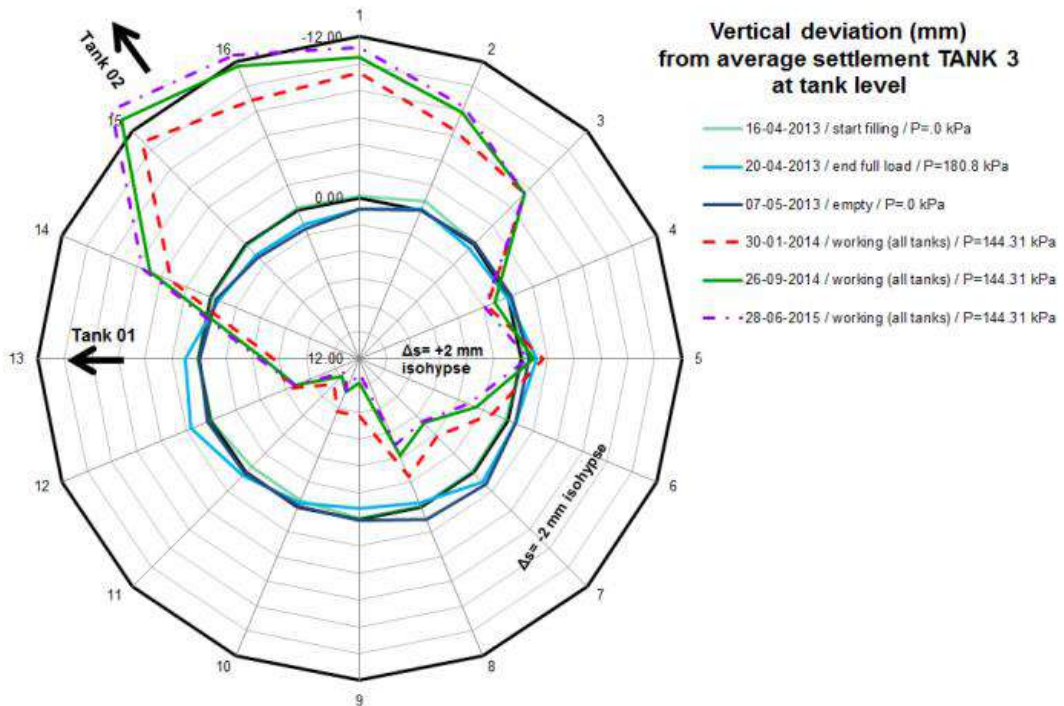


Figure 27 Vertical deviation from average settlement (mm) of Tank 3 - during hydro test and during operation, at tank level.

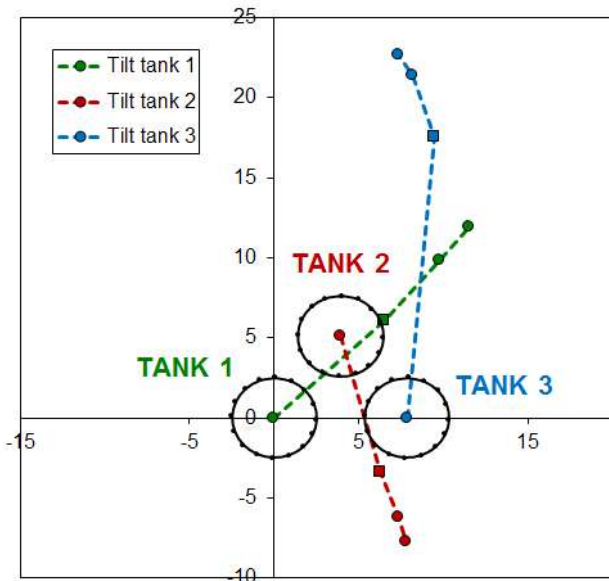


Figure 28 Direction and size (mm) of tilt of the tanks during operation.

An increased value of the tilt compared to the situation of the hydro-test is also to be expected due to the interaction of the different loads. Although the average settlement for all tanks is very similar, there is a significant difference in the size and direction of the tilt. Both tank 1 and 2 exhibit about 15mm of nearly perfectly planar tilt (0.00031 m/m) towards the central area in-between the tanks (i.e. the centre of the stress field), while tank 3 tilts clearly slightly distorted and almost directly north for about 22 mm (0.00046 m/m). The local subsoil heterogeneities below tank 3 are probably the reason for such uneven tilt of tank 3.

Akhavan-Zanjani (2009) reviewed a large number of case studies and references related to allowable settlement criteria for large diameter steel tanks as in Ostend. A possible outcome from all of this could for example lead to a maximum allowable differential settlement of $0.004D$ and an ultimate tilt of $0.007H$ (where D and H are respectively the diameter and the height of the tank).

The values of average settlement, tilt and distortion measured so far are therefore, in our case, still well below such critical values.

3.3 Tank tilt at “tank level” vs “foundation level“ (during hydro test)

The rotation or tilting of the foundation slab as measured during the hydro loading tests has been summarized – from the Tables 2, 3 and 4 (measured points at foundation level) – for the major loading conditions, in the Figure 29 to 31.

The first conclusion can be that after all, all tank foundation slab tilting values do remain very low; as such not more than 3 to 4 mm over a tank diameter of 48 m; so a rotation as low as $<1/12000$, higher than the $1/16000$ above, at tank level, due to the interaction of the tank and foundation through the interlayer of asphalt and due to different interaction of the outside temperature (sun shine) on the perimeter in the Eastern – Southern part of the tanks.

It would seem that some higher and apparently uneven tilt was measured at foundation level rather than at tank level during the hydro testing. Tilting at foundation level is clearly influenced by the interaction of the tank loading schemes, as for example for tank 02 in Figure30. The reference line of the tank 02 slab condition when start filling was measured at the time (on 05/04/2013) of full loading of tank 01. The unloaded foundation slab plain of tank 02 therefore was already tilting 4 mm towards the tank 01 at the start of the filling of tank 02. It means that the tilting shown in Figure 30 (lines at full load, end load and empty tank) all start from an inclined plain towards tank 01. So, the downward tilt of -3 mm of perimeter point 3 at full loading conditions of tank 02, is no more than a back tilting of the initial upheave the foundation slab plain had at that point 3 due to the tank 01 influence. Similarly, the upward tilting of perimeter point 11 by some 1.8 mm at full loading of the tank 02 is induced by the back tilting of the entire foundation slab from the initial condition influenced by tank 01. The remaining tilt of tank 02 at the empty tank condition, in this respect is reflecting a more or less horizontal tank slab after full unloading, when interpreting these data with the initial tilting of the slab plain.

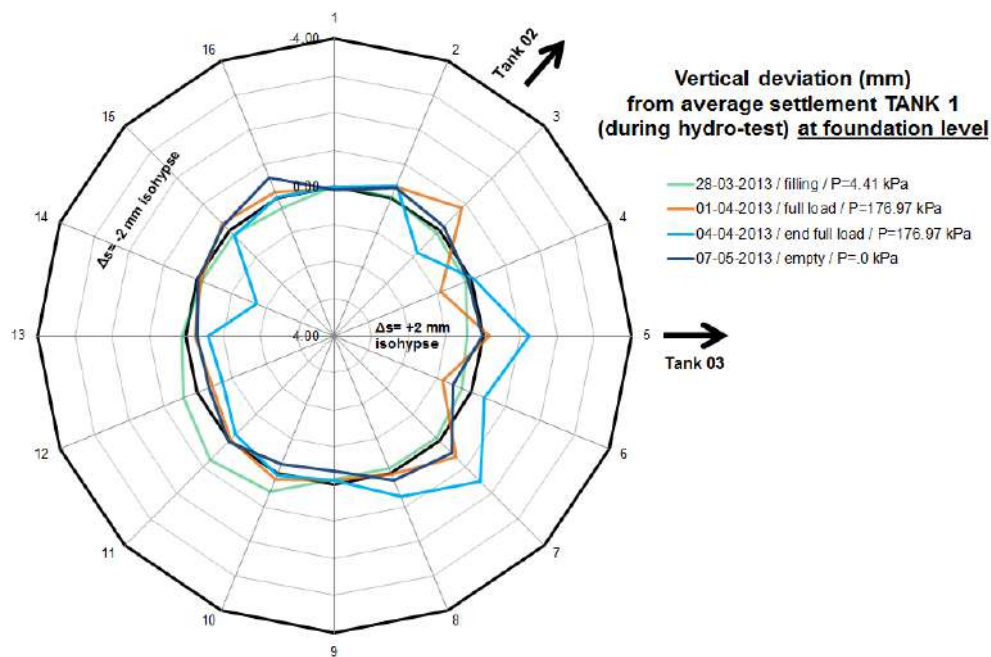


Figure 29 Vertical deviation from average settlement (mm) of Tank 1 - during hydro test (Tanks 02 and 03 still empty), at foundation level.

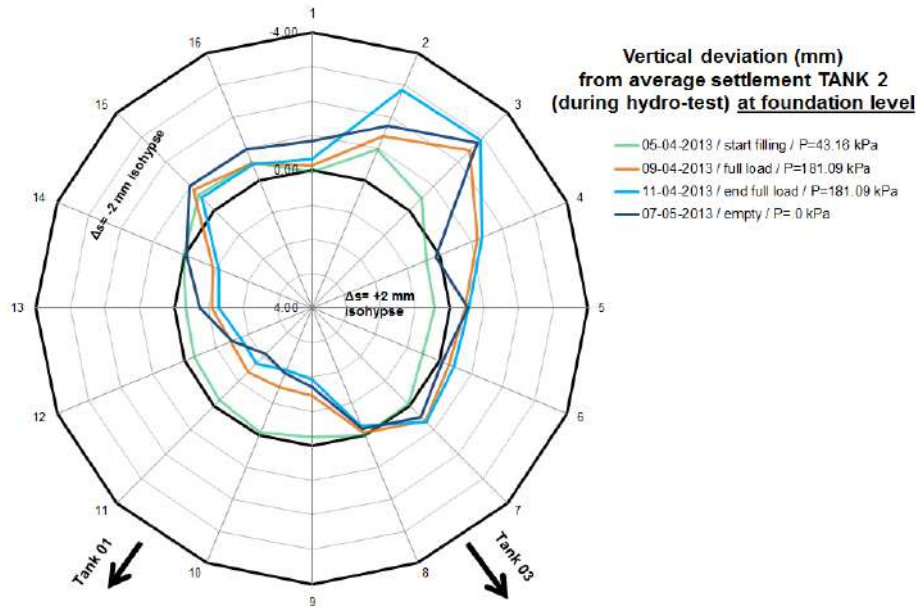


Figure 30 Vertical deviation from average settlement (mm) of Tank 2 - during hydro test, at foundation level.

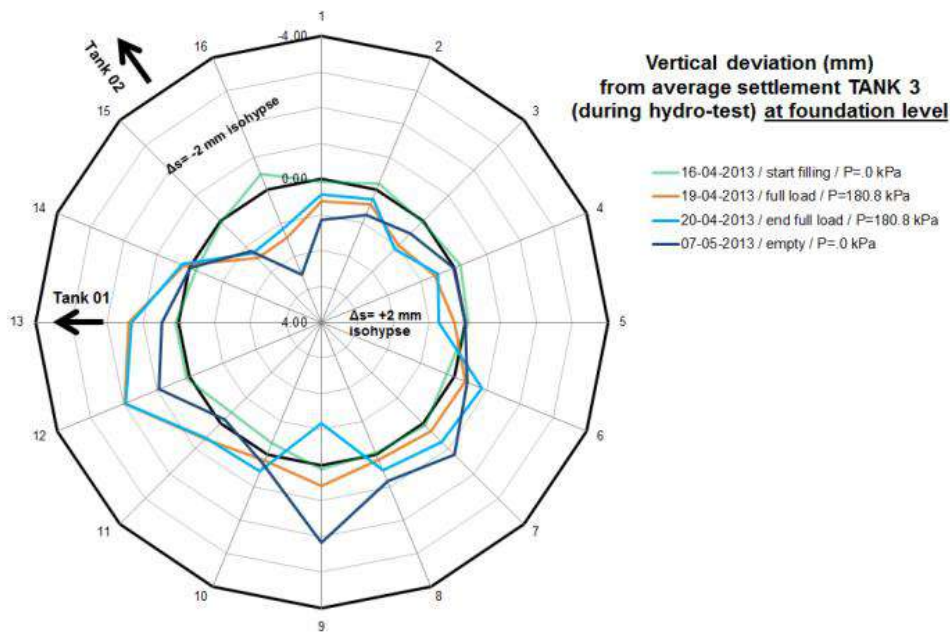


Figure 31 Vertical deviation from average settlement (mm) of Tank 3 - during hydro test, at foundation level.

The foundation slab of Tank 03 had much less initial tilting (on 16/04/2013) due to the influence of the tanks 01 and 02; the soil conditions at the location of tank 03 being rather different from the rest of the tank site. The initial tilting towards tank 01 of the foundation slab was not more than about 1 mm. It means that the reference line in the Figure 31 is indicating a slightly tilted foundation slab of tank 03 towards tank 01 (at the start of filling, being tanks 01 and 02 already empty at that moment – cfr Figure 22). The remaining tilt after full unloading of the tank 03 therefore (cfr Figure 31) is higher than for the tanks 01 and 02; but after all not more than about 2.5 mm toward the South. This can again be attributed to the much more heterogeneous soil conditions at this location; it means quite variable stiffness distributions in the foundation soil.

When comparing then the vertical deviation from average settlement as measured during the hydro test at foundation level and at tank level, there certainly is an equalizing interactive beneficial

effect of the asphalt layer in between the steel tank bottom and the foundation slab.

4. ANALYSIS OF THE TIME SETTLEMENT BEHAVIOR

The settlement of the full pile group is only marginally influenced by the fill material. The important characteristics are those from the dense sand layer, the silty clay and, in the long term, the thick OC clay layer.

Unfortunately, as mentioned before, the data on the two latter are very limited. Authors therefore have attempted to analyze the current settlement data in order to predict the long term behaviour of the construction.

Based on the analysis of the CPT data, following data on the constrained modulus were derived (Robertson 2010) as shown in Table 8.

Based on the compressibility parameters out of the CPT data and the immediate compressibility parameters derived from the fast

hydro-test, a single value of the consolidation coefficient c_v for the silty clay was calculated to obtain the best fit between predicted and measured average settlements.

Table 8 Estimated deformation parameters from CPT.

layer	M (constrained modulus)
sand	170-209 MPa
silty clay	$27 + 2*(z-24)$ MPa between 24-44m depth

The prediction was done using a simplified 3D elastic stress model (again using the SteinP 3DT program). Referring to some representative grid-points, we have first considered the deformation with time from the loading of each separate tank and then we have added together the three different distributions in accordance to the superposition effect. Of course, when adding together the settlement distribution of each tank, we took into account the fact that the three tanks have not been loaded all at the same time but in a timeframe of 6 months. The model takes also into account the slight lower thickness of the sand layer below tank 3.

The ultimate average settlement for the tanks ranges from 87 to 90 mm and the centers of the tank settle 132 to 136mm (Figure 32). The long-term tilt ranges from 19 to 21 mm.

As the actual size of the consolidating layer is unknown, fitting was done on the basis of the combined c_v/d^2 parameter (where d is the drainage path length). This leads to a value of the time factor c_v/d^2 of $0.0023 \text{ month}^{-1}$.

The results of the fitting are presented in Figures 33 and 34, which show the predicted versus measured values for respectively the average settlement and tilting of the tanks. The time range which is presented is approximately 20 years.

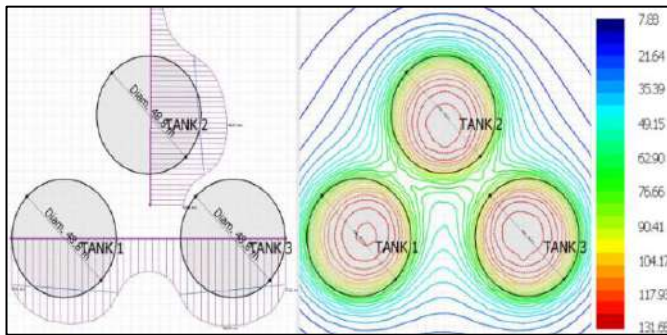


Figure 32 Simplified settlement analysis of the tanks under operational load.

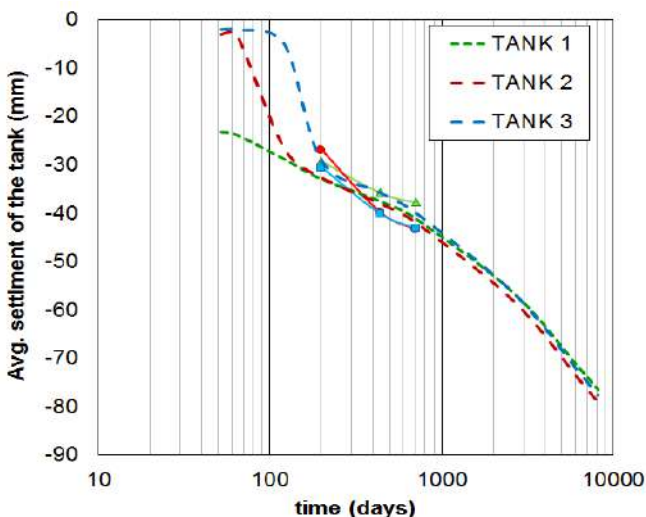


Figure 33 Predicted (lines) versus measured (dots) average settlement of the tanks under operational load.

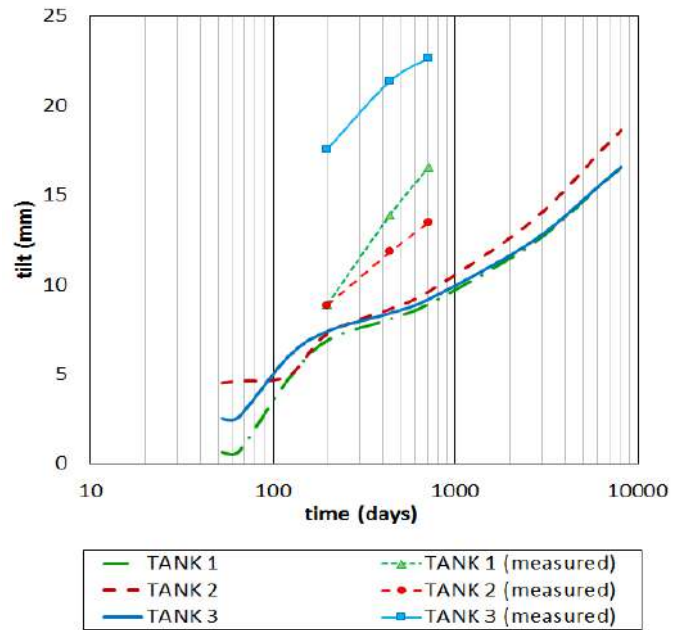


Figure 34 Predicted (lines) versus measured (dots) tilt of the tanks under operational load.

The prediction at this point underestimates the amount of tilt which is occurring, especially for tank 3. This could be due to the existence of some stiffness heterogeneity in the region of this tank, which could also be responsible for the distortion (non-planar tilt).

Further modelling would require additional soil data to increase the accuracy of the soil model and higher-level software capable of taking into account complex soil layering.

5. CONCLUSIONS

The load-settlement analysis of the pile group measured data, in prediction based on the instrumented single pile load test up to “failure”, are showing the useful potential of such simple prediction methods quite well. The data of the hydro tested oil tanks do illustrate that the end bearing displacement screw pile group underneath each 3 of the tanks, although in an almost 18 m very heterogeneous soil layering, can guarantee the quite uniform settlement of each of the tanks to a very similar level, governed by the stiffness of the bearing sand layer and the thick slightly OC clay layer underneath. At loading level somewhat less than 200 kPa, the overall settlement range is of the order of 20 mm in the hydro-test elastic settlement period of time.

During the hydro-test, the settlement trough starts already to develop by the mutual interaction of the 3 tanks at short distance from each other. The monitoring data during operation show anyhow such interaction much more clearly as the combined loading of the three groups gives rise to larger settlements than those measured during the separate loading of the hydro-tested tanks. Moreover, a significant increase of the tilt of the tanks occurs as well during operation.

Due to the large scale of the combined constructions, the influence depth is considerably larger than the extent of the soil investigation. The tanks are underlain by very thick sandy clay and OC clay layers, which will govern the long term settlements. Authors have made an attempt to analyse the data obtained during the hydro-test and the current operational stage to make an educated guess on compressibility and consolidation coefficients. The obtained values lie within the normal range for these type of soils, and allow further extrapolation of the current measurements.

Additional measurements campaigns will take place in the next months to allow further optimization of the model.

6. REFERENCES

- Akhavan-Zanjani, A. (2009) "Settlement criteria for steel oil storage tanks". *EJGE*, Vol.13.
- Fellenius, B.H. (2001) "From strain measurement to load in an instrumented pile", *Geotechnical News*.
- Fellenius, B.H. (2002) "Determining the Resistance Distribution in Piles, Part I: Notes on Shift of No-Load Reading and Residual Load". *Geotechnical News Magazine* 20(2), 35-38.
- Fellenius, B.H. (2014) "Discussion on: an instrumented screw pile load test and connected pile group load-settlement behaviour by Van Impe et al. 2013". *Journal of Geo-Engineering Sciences* 1(2), 101–108.
- Robertson, P.K. (2010) "Soil behavior type from the CPT: An update". *Proceedings of International Symposium on Cone Penetration Testing, CPT10*.
- Robertson, P.K. (1990) "Soil classification using the cone penetration test". *Canadian Geotechnical Journal* 27(1), 151–158.
- Van Impe, P.O., Van Impe, W.F., Manzotti, A. and Seminck, L. (2015) "Load-settlement behaviour of three pile groups: a case study". *Proceedings XVI ECSMGE, Edinburgh*.
- Van Impe et al. (2013) "Discussion of an instrumented screw pile load test and connected pile group load settlement behaviour". *Journal of Geo-Engineering Sciences* 1(1), 13–36.
- Van Impe, W.F. et al. (1988) "Prediction of the single pile bearing capacity in granular soils out of CPT results". *Proceedings First International Symposium on Penetration Testing ISOPT I, (specialty session)*.
- Van Impe, W.F. et al. (1988) "End and shaft bearing capacity of piles evaluated separately out of static pile loading test results". *Proceedings of the First International Geotechnical Seminar Deep Foundations on Bored and Auger Piles*, 489-498. CRC Press/Balkema, Ghent.